Annals of Biomedical Engineering, Vol. 37, No. 1, January 2009 *(© 2008)* pp. 64–81
DOI: 10.1007/s10439-008-9585-x

Heart Rhythm and Cardiac Pacing: An Integrated Dual-Chamber Heart and Pacer Model

JIE LIAN and DIRK MÜSSIG

Micro Systems Engineering, Inc., 6024 SW Jean Road, Lake Oswego, OR 97035, USA

(Received 8 May 2008; accepted 10 October 2008; published online 18 October 2008)

Abstract—Modern cardiac pacemaker can sense electrical activity in both atrium and ventricle, and deliver precisely timed stimulations to one or both chambers on demand. However, little is known about how the external cardiac pacing interacts with the heart's intrinsic activity. In this study, we present an integrated dual-chamber heart and pacer (IDHP) model to simulate atrial and ventricular rhythms in the presence of dual chamber cardiac pacing and sensing. The IDHP model is an extension and improvement of a previously developed open source model for simulating ventricular rhythms in atrial fibrillation and ventricular pacing. The new model takes into account more realistic properties of atrial and ventricular rhythm generators, as well as bi-directional conductions in atrium, ventricle, and the atrio-ventricular junction. Moreover, an industry-standard dual-chamber pacemaker timing control logic is incorporated in the model. We present examples to show that the new model can generate realistic cardiac rhythms in both physiologic and pathologic conditions, and simulate various interactions between intrinsic heart activity and extrinsic cardiac pacing. Among many applications, the IDHP model provides a new simulation platform where it is possible to bench test advanced pacemaker algorithms in the presence of different types of cardiac rhythms.

Keywords—Dual-chamber, Cardiac pacemaker, Sensing, Pacing, AV junction, Arrhythmia.

INTRODUCTION

The heart has a unique electrical system that controls the rhythm of the heartbeat. In a healthy heart, the sinoatrial node in the right atrium serves as the natural pacemaker, generating rhythmic electrical pulses that spread across both atria. These electrical pulses are delayed at the atrio-ventricular (AV) junction, or AVJ, before traveling along left and right bundle branches and exciting both ventricles (Fig. 1). It is well known that structural or functional abnormalities of the cardiac electrical conduction system can lead to cardiac arrhythmias.

First invented about a half-century ago, the implantable cardiac pacemaker is a medical device designed to regulate the heartbeat. It can monitor the intrinsic heart rhythm, and deliver pacing pulses to proper heart chamber(s) when needed. Modern cardiac pacemaker can also adjust the pacing rate according to patient's metabolic demand, time pacing sequence to synchronize the contraction of multiple chambers, trigger special pacing algorithm to terminate arrhythmic episodes or prevent their occurrence, among many other features.[22] The dual-chamber pacemaker is the most common type of pacemaker implanted today.[19] Connecting to an atrial lead and a ventricular lead, a dual-chamber pacemaker senses electrical signals in both right atrium and right ventricle, and paces one or both chambers if needed (Fig. 1).

For the native heart rhythm and the artificial pacemaker to form a close-loop system and coordinate their functions, complex interactions are expected. From sensing perspective, intrinsic heart activity may be detected by the pacemaker, or it may not be seen by the device if it falls into pacemaker blanking window or if the signal amplitude is smaller than the predefined sensing threshold (i.e., under-sensing). Other sensing problems, such as far-field sensing, T wave over-sensing, noise sensing, etc., have also been well known in the pacemaker industry. From pacing perspective, a pacing pulse is designed to capture the target heart chamber. Alternatively, it is also possible that the pacing fails to depolarize the heart if the stimulation strength is below the physiological capture threshold, or if the heart is still refractory due to an earlier excitation. Things become more complicated when both sensing and pacing are considered. For example, device sensing of intrinsic cardiac signal may inhibit the pacing output, whereas device pacing may pre-excite the myocardium and suppress its intrinsic rhythm.

Address correspondence to Jie Lian, Micro Systems Engineering, Inc., 6024 SW Jean Road, Lake Oswego, OR 97035, USA. Electronic mail: jie.lian@biotronik.com

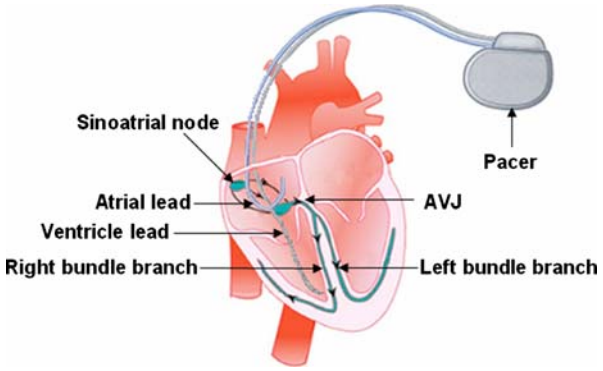

FIGURE 1. Illustration of the cardiac electrical conduction pathway and an implantable dual-chamber cardiac pacemaker connecting with a right atrial lead and a right ventricular lead.

Furthermore, when both intrinsic depolarization and paced depolarization are present, fusion of activation waves is possible.

PRIOR WORK

Ironically, despite the progress of cardiac arrhythmia research and the advance of the pacemaker technology, so far there is no computer model that can realistically simulate how the external pacemaker interacts with the heart's intrinsic rhythm.

Early efforts had focused on modeling RR intervals in atrial fibrillation (AF), likely reflecting both its clinical significance and its perplexing 'irregularly irregular' ventricular rhythm. The variation of RR intervals during AF has been attributed to unstable electrophysiological properties of both atrial source and AVJ.[3] As a convenient mathematical assumption, the arrival of 'random' AF impulses has been conventionally modeled as a Poisson process.[4,7,18] The modeling of AV conduction, however, has been a matter of debate for decades.

Concealed conduction models have been traditionally used to explain the ventricular response in AF.[10,18] However, theoretical analysis showed that these simplified models could not adequately account for various patterns of RR interval histograms observed experimentally.[4] Wittkampf *et al.* proposed a different model in which the AVJ functions as a pacemaker whose rate and rhythm are modulated by AF impulses,[24,25] but this hypothesis was later rejected by an experimental validation.[23] An alternative model was developed by Meijler *et al.*, who believed that electrotonic modulation of AV conduction by concealed impulses is responsible for the irregular RR intervals in AF.[17] Nonetheless, the inverse relationship between atrial and ventricular rates in AF predicted by this model was not confirmed in a clinical study.[2]

Treating the AVJ as a lumped structure with defined electrical properties, Cohen *et al.* developed another computer model, which they showed could account for most principal statistical properties of the RR intervals during AF.[4] In a different approach, Glass's group developed several models to characterize the nonlinear dynamics of AV conductions or statistical properties of RR intervals.[11,21,26] Although all these models could provide reasonable estimate of RR interval output for a given AF input, cardiac pacing was not considered thus its effect on intrinsic rhythm could not be addressed.

Recently, we have developed an AF–VP model to elucidate the effects of ventricular pacing (VP) on the ventricular rhythm in AF.[12] This model can be viewed as an extension and enhancement of Cohen's model, by taking into account VP, rate-dependent AV conduction and AV refractoriness, and electrotonic modulation in the AVJ. It has been demonstrated that this model could explain most experimental observations, including various patterns of RR interval distribution in AF,[12] biphasic relationship between atrial and ventricular rates in AF,[12] and the rate stabilization effects of VP.[12,14,15] We have further validated this model through simulated atrial pacing protocols, which are simpler-case scenarios by factoring out the randomness of AF and the interactions with VP.[13] To facilitate the use and further improvement of the AF–VP model, its software has been made freely available on PhysioNet (http://www.physionet.org/physiotools/afvp/).[6] The software architecture and design of the computer model have also been provided in an open access format.[16]

AIM OF STUDY

Although the AF–VP model can simulate many types of cardiac rhythms in both physiological and pathological conditions,[12–14] it does not support more advanced simulations involving dual-chamber cardiac pacing and sensing. The availability of such a computer model would not only facilitate cardiac rhythm analysis in pacemaker patients, but also make it possible to bench test various embedded pacemaker algorithms and guide the development of novel device features for cardiac rhythm management.

In this study, we present a new simulation framework called integrated dual-chamber heart and pacer (IDHP) model, which is an extension of the AF–VP model by incorporating more realistic heart rhythm generators, bi-directional wave conductions, and an industry-standard dual-chamber pacemaker timing control logic. As demonstrated below, the IDHP model provides an abstract yet realistic

representation of the native cardiac electrical conduction system and its interactions with external cardiac pacing.

MODEL STRUCTURE

Figure 2 shows the schematic diagram of the IDHP model structure, which consists of 8 interconnected modules: (1) atrial source, (2) ventricle source, (3) atrial conductor, (4) ventricle conductor, (5) AVJ, (6) atrial lead, (7) ventricle lead, and (8) pacer. As illustrated in the figure and described below, bi-directional couplings exist between different modular pairs.

Atrial Source Module

The atrial source module maintains an atrial rhythm generator, which supports generating different types of intrinsic atrial impulses, including sinus rhythm (with fixed atrial intervals, or random atrial intervals with predefined probability distribution); AF rhythm (e.g., Poisson distribution of impulse arrival rate and varying impulse strength); atrial ectopic rhythm (with predefined incidence probability and random atrial coupling interval); and custom rhythm (i.e., import atrial intervals from external files representing preselected atrial rhythms).

An impulse output from the atrial rhythm generator can start an antegrade wave (toward AVJ) in the atrial conductor. Meanwhile, it provides input to the atrial lead for atrial sensing (AS). On the other hand, the atrial rhythm generator is reset by either a retrograde wave (escaping from AVJ) in the atrial conductor, or a supra-threshold atrial pace (AP) delivered by the atrial lead. In addition, the atrial source module can also generate exogenous atrial noise (with defined incidence probability), which can be sensed by the atrial lead, but cannot generate activation wave in the atrial conductor nor reset the atrial rhythm generator.

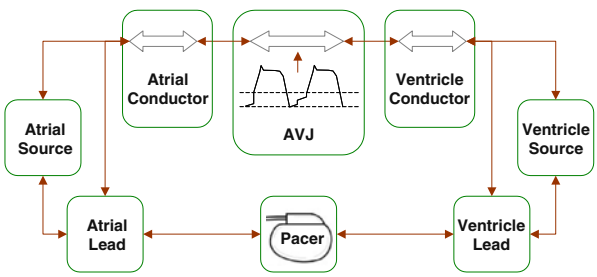

FIGURE 2. Schematic diagram of the IDHP model structure.

Ventricle Source Module

The ventricle source module maintains a ventricle rhythm generator, which can generate two types of intrinsic ventricular impulses: ventricular escape rhythm (with fixed or random intervals which are usually long to simulate slow escape rate, but can be short to simulate ventricular tachyarrythmia); and ventricular ectopic rhythm (with predefined incidence probability and random ventricular coupling interval).

An impulse output from the ventricle rhythm generator can start a retrograde wave (toward AVJ) in the ventricle conductor. Meanwhile, it provides input to the ventricle lead for ventricular sensing (VS). On the other hand, the ventricle rhythm generator is reset by either an antegrade wave (escaping from AVJ) in the ventricle conductor, or a supra-threshold VP delivered by the ventricle lead. In addition, the ventricle source module can also generate exogenous ventricle noise (with defined incidence probability), which can be sensed by the ventricle lead, but cannot generate activation wave in the ventricle conductor nor reset the ventricle rhythm generator.

Atrial Conductor Module

The atrial conductor module supports simulation of bi-directional atrial conductions. An atrial activation wave (antegrade or retrograde) will not be initiated unless the atrial conductor completes a predefined atrial refractory period since its last activation.

The antegrade atrial conduction is started by either an atrial rhythm generator output or a captured AP, and is terminated after the antegrade wave hits the AVJ, or collides with a retrograde atrial conduction wave (atrial fusion). Conversely, the retrograde atrial conduction is started after the completion of a retrograde AV conduction (escaping from AVJ), and is terminated after the retrograde wave conducts to atrial rhythm generator or collides with an antegrade atrial conduction wave (atrial fusion).

Ventricle Conductor Module

The ventricle conductor module supports simulation of bi-directional ventricular conductions. A ventricular activation wave (antegrade or retrograde) will not be initiated unless the ventricle conductor completes a predefined ventricular refractory period since its last activation.

The antegrade ventricular conduction is started after the completion of an antegrade AV conduction (escaping from AVJ), and is terminated after the antegrade wave conducts to ventricle rhythm generator, or collides with a retrograde ventricular conduction wave (ventricular fusion). Conversely, the retrograde

ventricular conduction is initiated by either a ventricle rhythm generator output or a captured VP, and is terminated after the retrograde wave hits the AVJ or collides with an antegrade ventricular conduction wave (ventricular fusion).

AVJ Module

The AVJ is modeled as a lumped structure with defined electrical properties, including automaticity, conductivity, and refractoriness.[4,12] The AVJ fires when its membrane potential (V_m) reaches the depolarization threshold (V_T). The activation of AVJ starts a refractory period, when the AVJ is refractory to any stimulation. At the end of refractory period, the AVJ membrane potential returns to the resting potential (V_R) and starts to rise in a linear manner. Each time an impulse (antegrade or retrograde) hits the AVJ during phase 4, its membrane potential is increased by a discrete amount (ΔV), which is dependent on the impulse strength.

The firing of AVJ generates an activation wave that starts an antegrade or retrograde AV conduction. If AVJ is retrograde activated while an antegrade wave has not finished its AV conduction or vice versa, a collision occurs, annihilating the activation waves in both directions. Both refractory period and conduction delay of the AVJ are dependent upon its recovery time (RT), which is defined as the interval between the end of last AVJ refractory period and the current AVJ activation time. Mathematically, the AV conduction delay (AVD) is modeled as[11,12,21,26]

$$AVD = AVD_{\min} + \alpha \exp(-RT/\tau_c) \tag{1}$$

where $AVD_{\min}$ is the shortest AVD when $RT \rightarrow \infty$, α is the longest extension of AVD when $RT = 0$, and τ_c is the conduction time constant. The AV refractory period (τ) is modeled as[4,12]

$$\tau = \tau_{\min} + \beta(1 - \exp(-RT/\tau_r)) \tag{2}$$

where $\tau_{\min}$ is the shortest τ corresponding to $RT = 0$, β is the longest extension of τ when $RT \rightarrow \infty$, and τ_r is the refractory time constant. In addition, the electrotonic modulation is also incorporated in the model, by assuming τ is prolonged by a concealed impulse according to[11,12,17]

$$\tau' = \tau + \tau_{\min}(t/\tau)^{\theta}[\min(1, \Delta V/(V_T - V_R))]^{\delta} \tag{3}$$

where τ and τ' are, respectively, the original and prolonged refractory periods, t is the time when the impulse is blocked ($0 < t < \tau$), and the degree of extension depends on the timing and strength of the blocked impulse, which are respectively modulated by two positive parameters θ and δ.

Atrial Lead Module

The atrial lead module supports simulation of both AP and AS.

An AP captures the atrium if the atrial conductor is non-refractory and the AP strength is greater than a predefined atrial threshold. The captured AP also resets the atrial rhythm generator, and starts an antegrade wave in the atrial conductor. On the other hand, no effect follows a non-capture AP.

The atrial lead senses any types of electrical signals in the atrium, which could be intrinsic atrial depolarizations (including atrial rhythm generator output and retrograde atrial activation), or exogenous noise (generated by the atrial source module).

Ventricle Lead Module

Similarly, the ventricle lead module supports simulation of both VP and VS.

A VP captures the ventricle if the ventricle conductor is non-refractory and the VP strength is greater than a predefined ventricular threshold. The captured VP also resets the ventricle rhythm generator, and starts a retrograde wave in the ventricle conductor. On the other hand, no effect follows a non-capture VP.

The ventricle lead senses any types of electrical signals in the ventricle, which could be intrinsic ventricular depolarizations (including ventricle rhythm generator output and antegrade ventricular activation), or exogenous noise (generated by the ventricle source module).

Pacer Module

Modern pacemakers maintain a plural of timers and windows to perform sense event classification and pace timing control. Most of these timing control logics are supported by the pacer module, such as the basic interval, pace and sense AV delays, atrial and ventricular blanking windows, atrial and ventricular refractory periods, upper tracking interval, far-field window, safety window, etc. Interacting with both atrial and ventricle leads, the pacer module classifies atrial and ventricular senses, and controls the timing of AP and VP, according to various industry-standard pacing modes, such as DDD, DDI, DVI, VDD, VVI, AAI, etc.[5] Some basic concepts on pacemaker timing are summarized in Appendix A.

The pacer module also provides support of continuous interval measurement, including but not limited to, the A–A intervals, the V–V intervals, the A–V intervals, the V–A intervals, etc., based on which the pacemaker can perform rate and rhythm analysis, log diagnostic statistics, and implement advanced pacing algorithms.

MODEL IMPLEMENTATION

Figure 3 shows the top-level flowchart of the IDHP model. The simulation reads model parameters from an external configuration file (see Appendix B), and then initializes model variables including various timers, flags, counters, etc. Some major timers associated with the heart modules and their start and stop conditions are listed in Table 1. Besides, the simulation maintains a plural of pacer specific timers (e.g., to schedule AP and VP, to start and stop various windows for sense classification, to measure intervals between different event types), which are mostly dependent on the pacing mode. The simulation runs at the predefined sampling frequency. At each sample time, the model updates its time-dependent variables (e.g., AVJ membrane potential, active timers), and then handles possible event(s) as detailed below. The simulation continues until a predefined number of cardiac beats are generated or the simulation time runs out, when the model logs statistics and exits.

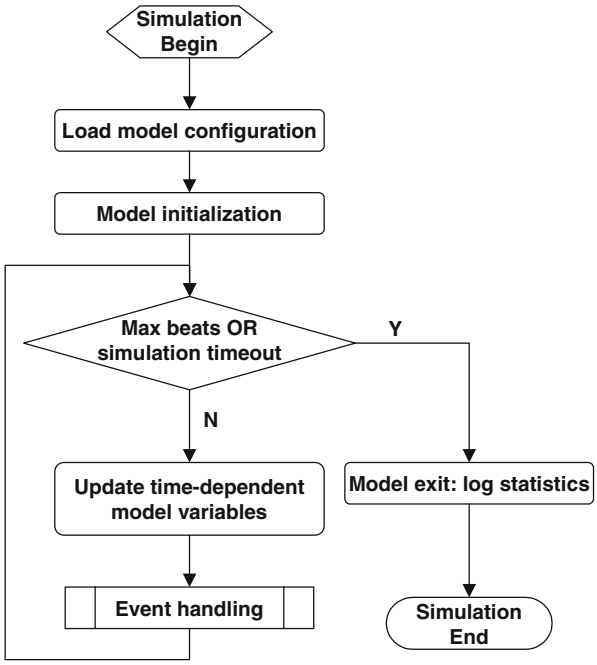

FIGURE 3. Top-level flowchart of running IDHP model simulation.

The general event handling routine is described in Fig. 4, in which the AP/AS handling and VP/VS handling are further illustrated in Fig. 5. The model checks its timers and status flags to detect various events and calls for respective service routines when necessary. Atrial or ventricular fusion (*AtrFusion* or *VtrFusion*) occurs when antegrade and retrograde waves meet in the atrium or ventricle, respectively. Completion of antegrade atrial conduction or retrograde ventricle conduction leads to antegrade or retrograde invasion of AVJ (*AnteHitAvj* or *RetrHitAvj*). An antegrade or retrograde activation wave escapes the AVJ (*AnteEscAvj* or *RetrEscAvj*) upon completing the respective AV conduction. The AVJ is activated (*ActivateAvj*) and becomes refractory (*StartAvjRef*) if its membrane potential exceeds its depolarization threshold, whereas the end of AVJ refractory period starts the phase 4 (*StartAvjPh4*). Pacer delivers AP or VP (*AtrPace* or *VtrPace*) according to programmed

TABLE 1. List of major timers associated with the heart modules of the IDHP model.

Timer	Start condition	Stop condition
Atrial rhythm generator timer	Impulse output from atrial rhythm generator, or atrial rhythm generator reset by AP or retrograde atrial conduction	Next impulse output of atrial rhythm generator, or atrial rhythm generator reset by AP or retrograde atrial conduction
Ventricle rhythm generator timer	Impulse output from ventricle rhythm generator, or ventricle rhythm generator reset by VP or antegrade ventricle conduction	Next impulse output of ventricle rhythm generator, or ventricle rhythm generator reset by VP or antegrade ventricle conduction
AVJ refractory timer	Begin of AVJ refractory period caused by AVJ activation	End of AVJ refractory period
Antegrade AVJ timer	Antegrade AVJ activation	Completion of antegrade AV conduction, or collision with a retrograde AV conduction
Retrograde AVJ timer	Retrograde AVJ activation	Completion of retrograde AV conduction, or collision with an antegrade AV conduction
Antegrade atrial timer	Start of antegrade atrial conduction caused by atrial rhythm generator output or a captured AP	Completion of antegrade atrial conduction, or collision with a retrograde atrial conduction
Retrograde atrial timer	Start of retrograde atrial conduction when a retrograde wave escapes the AVJ	Completion of retrograde atrial conduction, or collision with an antegrade atrial conduction
Antegrade ventricle timer	Start of antegrade ventricle conduction when an antegrade wave escapes the AVJ	Completion of antegrade ventricle conduction, or collision with a retrograde ventricle conduction
Retrograde ventricle timer	Start of retrograde ventricle conduction caused by ventricle rhythm generator output or a captured VP	Completion of retrograde ventricle conduction, or collision with an antegrade ventricle conduction

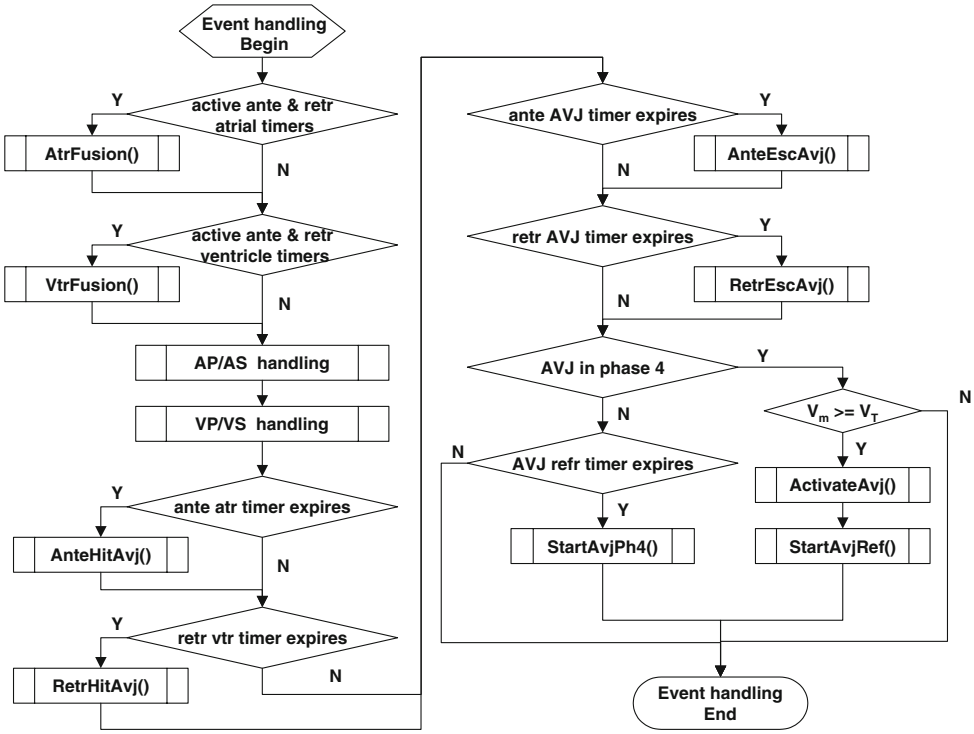

FIGURE 4. General event handling routines implemented in IDHP model.

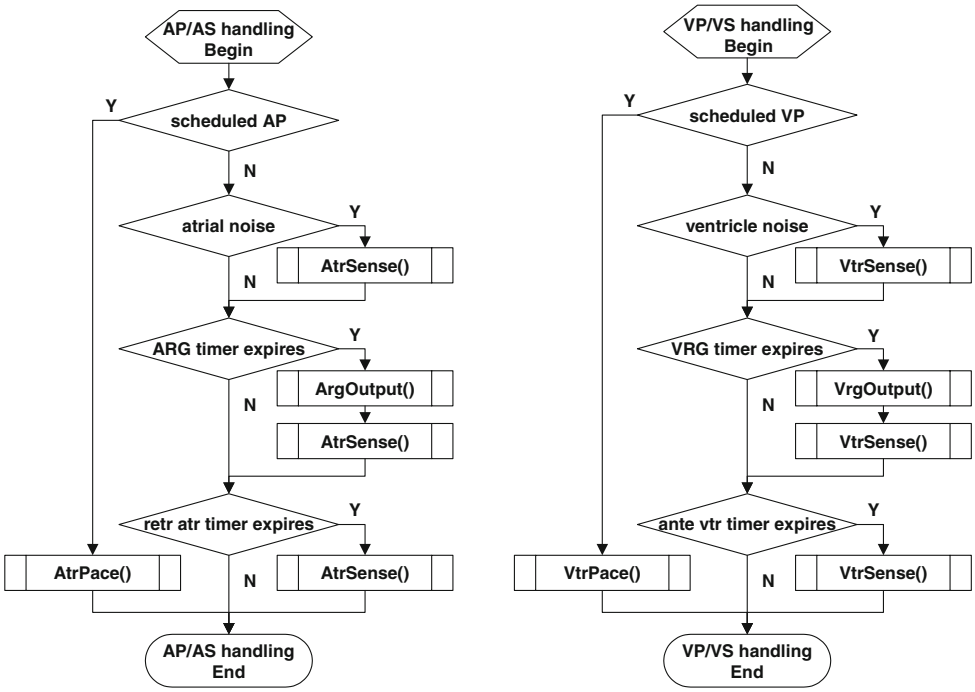

FIGURE 5. Specific event handling routines implemented in IDHP model for AP/AS events (left) and VP/VS events (right).

timing logic. Atrial sense (*AtrSense*) can be caused by atrial rhythm generator output (*ArgOutput*), retrograde atrial activation, or atrial noise, whereas ventricle sense (*VtrSense*) can be the result of ventricle rhythm generator output (*VrgOutput*), antegrade ventricle activation, or ventricle noise. More detailed flowcharts of IDHP model event handling are shown in Appendix C.

RESULTS

By changing model parameters through the configuration file (see Appendix B), the IDHP model can simulate various types of heart rhythm in the presence of dual-chamber cardiac pacing and sensing.

As examples, Figs. 6–11 show some representative segments of the model generated event markers. In these figures, sense and pace events are represented by vertical bars; atrial events are plotted in the upper area and ventricular events are plotted in the lower area. Each vertical bar has a symbol representing event type classified by the pacer: pace (circle), sense (triangle), refractory or far-field sense (star), and undetected due to blanking (cross). Pace amplitudes (unit: V) are shown next to the pace markers. In addition, the following marker annotations are used to show the true event type: I—intrinsic depolarization; E—ectopic depolarization; R—retrograde atrial depolarization; S—conducted ventricular depolarization; C—captured pace; L—loss-of-capture pace.

Figure 6 shows a segment of model generated event markers when the heart is in normal sinus rhythm and the pacer operates in DDD mode. In this example, the

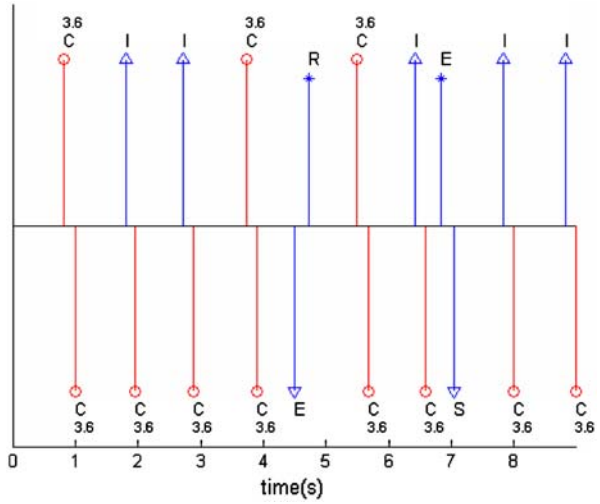

FIGURE 6. An exemplary segment of model-generated event markers when the heart is in normal sinus rhythm with incidental atrial extra-systole and ventricular extra-systole, and the pacer operates in DDD mode.

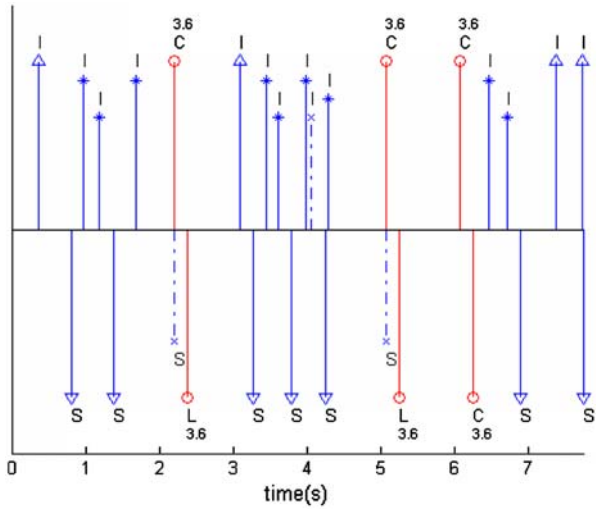

FIGURE 8. An exemplary segment of model-generated event markers when the heart is in AF rhythm while the pacer operates in DDI mode.

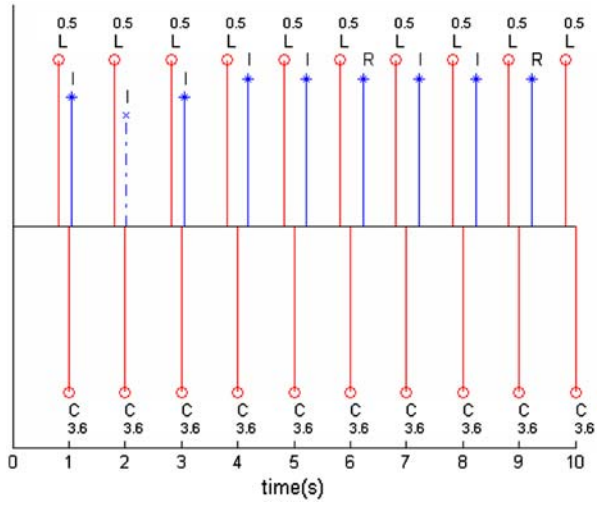

FIGURE 7. An exemplary segment of model-generated event markers when the heart is in normal sinus rhythm, and the pacer operates in DDD mode but with sub-threshold AP amplitude.

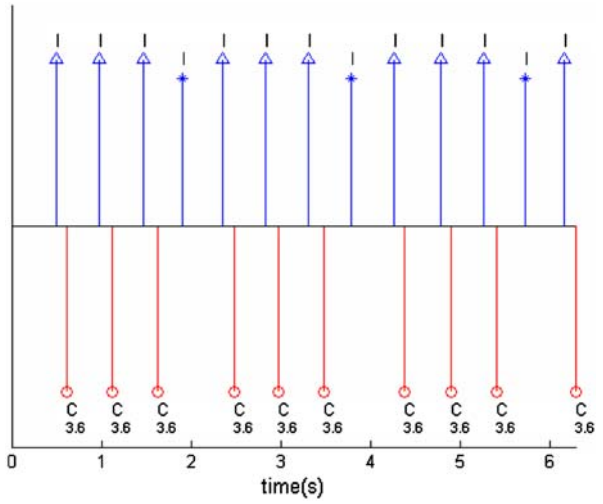

FIGURE 9. An exemplary segment of model-generated event markers when the heart is in atrial tachycardia rhythm, and the pacer operates in DDD mode but the VP rate is limited by the programmed upper tracking rate.

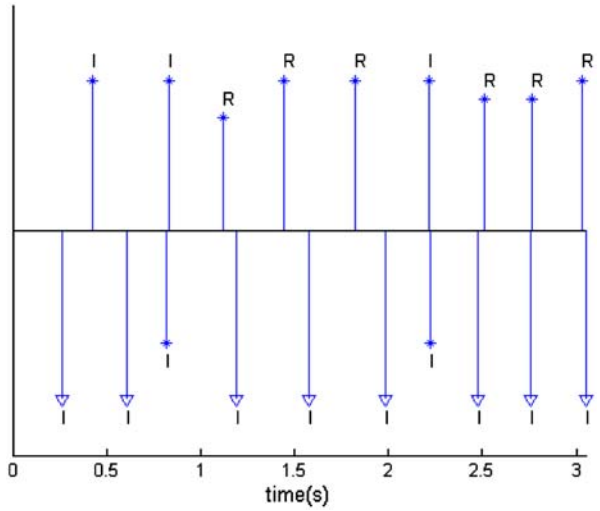

FIGURE 10. An exemplary segment of model-generated event markers when the heart is in ventricular tachycardia rhythm while the pacer operates in DDD mode.

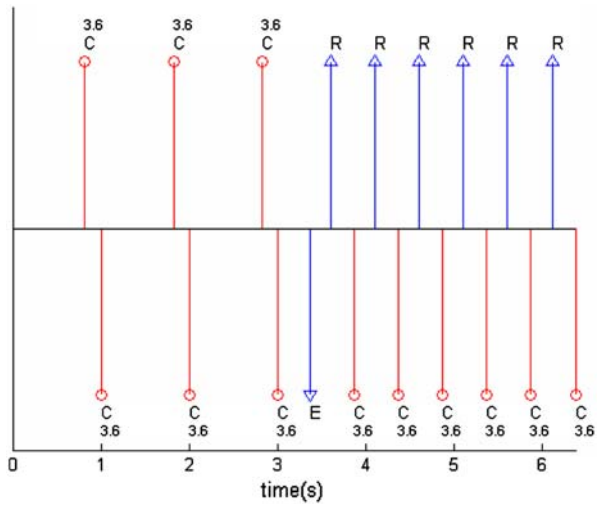

FIGURE 11. An exemplary segment of model-generated event markers representing pacemaker-mediated tachycardia in DDD mode.

intrinsic sinus rate (about 60 beats/min) is similar to pacer's basic rate (fixed at 60 pulses/min), thus the atrial rhythm is mixed between paces and senses. After four ventricular paces, a ventricular ectopic beat occurs, followed by a retrograde atrial depolarization. Two cycles later, an atrial ectopic beat occurs, followed by a conducted ventricular depolarization.

Similarly, Fig. 7 shows another segment of model generated event markers when the heart is in normal sinus rhythm and the pacer operates in DDD mode. However, in this example, the AP amplitude (0.5 V) was set below the atrial threshold (1.0 V). Because the sub-threshold AP does not capture the atrium, the sinus rhythm is preserved, evidenced by intrinsic atrial depolarization shortly after each AP (undetected by the pacer due to post-AP blanking, or detected as a far-field or refractory sense); or alternatively, the atrium is activated by retrograde conduction induced by VP.

Figure 8 shows a segment of model generated event markers when the heart is in AF rhythm and the pacer operates in DDI mode (as during pacemaker mode switch). The AF rhythm is characterized by random arrival of atrial impulses and irregular ventricular response. Evidently, some AF impulses are blocked and not conducted to the ventricle. Also note that the first two VPs fail to capture the ventricle despite their supra-threshold (threshold 1.0 V) pacing amplitude (3.6 V). As shown in the figure, each of the non-capture VP is immediately preceded by a conducted ventricular depolarization (but undetected by the pacer due to post-AP blanking) that renders the ventricle refractory.

Figure 9 shows an example of model simulated atrial tachycardia rhythm while the pacer operates in DDD mode. In this example, the atrial rate (about 126 beats/min) is slightly higher than the pacer upper tracking rate (fixed at 120 pulses/min). As expected, each normal AS is tracked by the pacer and followed by a VP. However, due to the limitation of the upper tracking rate, VP is postponed and can only be delivered at the end of the upper tracking interval. This causes progressive lengthening of the AS–VP interval, until an AS falls into the post-ventricular atrial refractory period (i.e., not tracked by the pacer), thus there is no following VP (i.e., periodic AV block). This is the well-known pacemaker Wenckebach behavior.[5]

Figure 10 shows an example of model simulated ventricular tachycardia rhythm while the pacer operates in DDD mode. Atrial tachycardia (intrinsic rate about 150 beats/min) is also simulated in this example (evidenced by three intrinsic AS events shown in the figure), but higher ventricular rate (about 200 beats/min) overdrives the ventricle and blocks antegrade AV conduction, and frequently entrains the atrium through retrograde VA conductions.

Finally, Fig. 11 shows a typical example of model simulated pacemaker-mediated tachycardia episode.[5] The model configuration for this example is similar to that of Fig. 6 except that the pacer's post-ventricular atrial refractory period is shortened. After three cycles of baseline AP–VP rhythm in DDD mode, a ventricular ectopic beat causes retrograde atrial depolarization, which is detected by the pacer as a normal AS. The pacer tracked this detected AS by delivering a VP at the programmed AV delay. The VP causes another retrograde AS, and the sequence repeats, leading to an endless loop tachycardia.

DISCUSSION

In this paper, we present a new IDHP model, which for the first time allows realistic simulation of heart rhythm in the presence of a dual-chamber cardiac pacemaker.

The IDHP model is an extension and improvement of the previous AF–VP model, which was shown to be able to explain many experimental observations in AF.[12] The AF–VP model was further validated through simulated atrial pacing protocols,[13] by reproducing most experimental results obtained in an isolated rat heart model.[8,9] Recently, the AF–VP model was also applied to elucidate the role of ventricular conduction time in rate stabilization for AF,[16] providing mechanistic explanation to the findings of a clinical study that found no measurable difference in rate stabilization effects between His bundle pacing and right ventricle apex pacing.[20]

Building on success of the AF–VP model, the IDHP model incorporates more realistic properties of the heart, including various rhythm generators (e.g., sinus rhythm, ectopic rhythm, escape rhythm, tachyarrhythmias, etc.), and bi-directional atrial, ventricular, and AVJ conductions. More importantly, the IDHP model encapsulates an industry standard pacer module that supports advanced timing control logic existing in state-of-the-art dual-chamber pacemakers. With these enhanced features, the IDHP model provides a unique platform to study complex interactions between intrinsic heart rhythm and extrinsic dual-chamber cardiac pacing. By adjusting model parameters, Figs. 6–11 provide clear, albeit certainly not exhaustive, examples of how the intrinsic heart rhythm would be affected by cardiac pacing, and how the cardiac pacemaker would sense, interpret and respond to the intrinsic heart activity.

Model Framework

It is clear from Fig. 1 that, in the IDHP model, the intrinsic heart rhythm generator, the cardiac conduction pathway, and the implantable cardiac pacemaker are integrated into a closed-loop system—as it is in the real world. The antegrade branch of the loop starts from the atrial source output, or from AP delivered by the pacer via the atrial lead. The resulting atrial depolarizations pass through the atrial conductor before bombarding the AVJ, where the signals are processed, then further propagate through the ventricle conductor, until reaching the ventricle source and being sensed by the pacer via the ventricle lead. On the other hand, the retrograde branch of the loop starts from the ventricle source output, or from VP delivered by the pacer via the ventricle lead. The resulting ventricular depolarizations pass through the ventricle conductor before penetrating the AVJ, where it is delayed before further invading the atrial conductor, until reaching the atrial source and being sensed by the pacer via the atrial lead. Evidently, multi-level interactions may occur between these two opposite electrical conduction branches.

The kernel component of the heart model is AVJ, which is treated as a hypothetical equivalent cell whose electrophysiological properties represent the overall behavior of all AV nodal cells.[4,12,16] A black-box modeling approach is used to characterize the input–output relationship of the AVJ: the input to the AVJ is the antegrade or retrograde invading impulses, while the output of the AVJ is the antegrade or retrograde activation waves conducting to the ventricle or atrium, respectively. Moreover, the functional behavior of the AVJ can be equated to multiple signal processing steps that involve blanking (refractory period), summation (phase 4), thresholding (activation), and time delay (AV conduction). From the system modeling perspective, the AVJ can also be regarded as a relay unit that connects its output (antegrade and retrograde activation waves) to the ventricle and atrium, which are, respectively, driven by two opposing electrical sources. The atrial source and the ventricular source compete for the activation of the AVJ, which serves as the common pathway for both antegrade and retrograde conductions.

Model Applications

The present model has a number of applications. First and foremost, the IDHP model provides a unique simulation environment to generate various cardiac rhythms, to emulate how the pacemaker would sense and classify cardiac events and then yield diagnosis, and moreover, to study how the cardiac pacing would affect the intrinsic cardiac rhythm. This makes it possible to rigorously bench test advanced pacemaker algorithms (in the presence of different heart rhythms and numerous variants, e.g., ectopic beat, noise, etc.) even before experimental or clinical investigations, thus may guide and speed up the development of novel device features for cardiac rhythm management.

Second, the IDHP model can help unravel many puzzling cardiac rhythms encountered in the real world. As demonstrated before, the AF–VP model can generate various patterns of normal and abnormal heart rhythms that are consistent with previous experimental observations.[12–14,16] Some seemingly conflicting observations could be explained in terms of a difference in model parameter settings.[12–14] With enhanced simulation capabilities, the IDHP model

offers a new tool to probe complex heart rhythms while taking into account dual-chamber cardiac pacing and sensing.

Third, the model provides an abstract yet realistic representation of the cardiac electrical conduction system including atrial and ventricular sources, and the atrium-AVJ-ventricle conduction pathway, all of which are under autonomic control. Many cardiac arrhythmias are thought to result from disturbances in autonomic modulation of the electrophysiological properties of the heart's electrical conduction system. Hence, the present model may become a useful tool to facilitate better understandings on the mechanisms of arrhythmia genesis, maintenance, and termination.

Last but not least, the model can contribute to the development of advanced biomedical signal processing techniques for cardiac arrhythmia research. For example, the present model can generate at least three closely coupled time series: PP (or A–A) intervals, RR (or V–V) intervals, and PR (or A–V) intervals. By simulating various cardiac rhythms, the model-generated time series can be used to build a standard test platform for quantitative evaluation or comparison of different signal processing techniques that have been developed for heart rhythm analysis.

Limitations and Future Work

This study is limited by the nature of computer simulation. Direct experimental validation of the model is certainly warranted to confirm its concrete behavior. Nonetheless, the IDHP model is a conceptual representation of: (a) the cardiac electrical conduction system with well-documented electrophysiological properties and (b) the dual-chamber cardiac pacing system whose technical features and control logics are clearly defined. The integration of these two systems allows rational encapsulation of cardioelectric and pacemaker variables, and the set of logical and quantitative relationships between them. Moreover, the validity of the model has also been demonstrated by its capability to account for most known experimental observations.[12–14]

Another limitation of the present study is that the model parameters are empirically defined. Ideally the parameters could be derived by fitting the model to experimental data, but a simultaneous search over all model parameters is technically impractical. Nonetheless, the dimension of the search space could be significantly reduced by deriving some baseline parameters independently. For example, the parameters pertaining to AV conduction time and refractory period may be derived from respective recovery curves, which can be obtained during application of standard atrial pacing protocols.[8] The parameters pertaining to electrotonic modulation may be found through a scanning process,[11] or estimated through more elaborate pacing protocols involving concealed conduction.[9] Other model parameters (e.g., AF frequency, relative impulse strength, and the rate of phase 4 depolarization) may be estimated by fitting the model with recorded RR interval distribution.[4]

Finally, further improvement of the IDHP model is planned for the future study. The architecture of the IDHP model is constructed in a modular manner. Such a modular design not only facilitates model change to achieve a particular purpose, but also allows potentially more realistic features of the heart and pacer to be included. For instance, it is highly attractive to enhance the heart model with autonomic modulation, which is known to significantly affect automaticity, excitability, and conductivity of the myocardial cells. The history-dependent behavior of the AV node, namely the fatigue and facilitation,[21] can also be incorporated into the present model by modifying the AV conduction formula. For the pacer model, more advanced device features and clinical problems (e.g., over-sensing, under-sensing, etc.) could be simulated. Besides, in view of the rapid progress in cardiac resynchronization therapy for treating refractory heart failure with cardiac dyssynchrony,[1] the next incremental step to build an integrated three-chamber (right atrium, right ventricle, left ventricle) heart and pacer model will be certainly challenging yet rewarding.

CONCLUSION

An integrated dual-chamber heart and pacer model is presented that enables realistic simulation of heart rhythm in the presence of a dual-chamber cardiac pacemaker. The detailed model structure is described within a unified yet flexible framework, where it is possible to study the interactions between intrinsic heart rhythm and extrinsic cardiac pacing. Representative examples are provided to illustrate the usage of the model, and its validity is demonstrated by its realistic outputs that are consistent with clinical observations. Further improvement of the model, as well as its scientific merits and potential applications are discussed.

APPENDIX A: BASICS OF PACEMAKER TIMING

Modern pacemakers have many therapeutic and diagnostic features, which are supported by hundreds of sophisticated pacer-specific timers and windows. While it is beyond the scope of this paper to discuss the

detailed pacemaker timing logic, the basic concept of dual-chamber pacemaker sensing and pacing is summarized below.

Figure A1 illustrates some common pacemaker windows used for device sensing. After each AP or VP, a blanking window is applied to the same channel and another blanking window is applied to the other channel to prevent device from sensing the pacing artifact. Any electrical event occurring in these blanking windows is not seen by the pacemaker. Each AP (or VP) also starts an atrial (or ventricular) refractory window, when an atrial (or ventricle) event can be seen, but usually is ignored by the pacemaker.

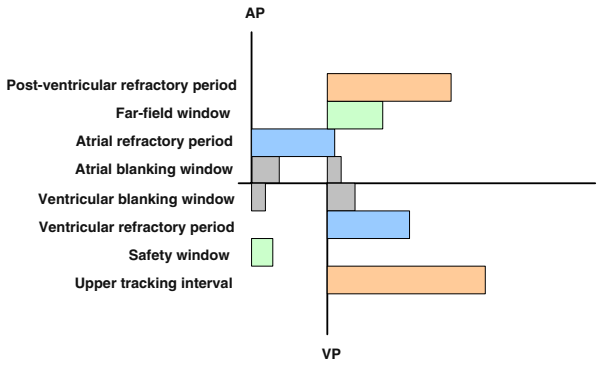

FIGURE A1. Schematic illustration of the pacemaker windows used for sensing.

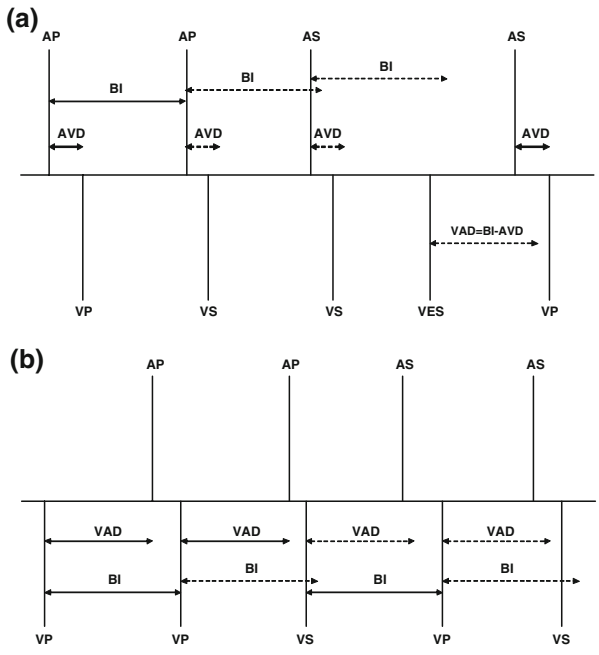

FIGURE A2. Schematic illustration of the pacemaker timing in (a) DDD mode and (b) DDI mode. BI: basic interval; AVD: AV delay; VAD: VA delay; VES: ventricular extra-systole.

A VP triggers both a far-field window and a post-ventricular atrial refractory period in the atrial channel. The former prevents far-field sensing of ventricular depolarization, and the latter prevents tracking of retrograde AS event that may lead to pacemaker-mediated tachycardia (see Fig. 11). On the other hand, an AP triggers a safety window in the ventricle channel. If an intrinsic ventricular activity is detected during this window (could not be differentiated from cross-talk), a VP will be triggered at the end of the safety window to prevent ventricular asystole. In addition, an upper tracking interval is applied after each VP, which sets the upper limit to the ventricular pacing rate in DDD mode (see Fig. 9). Similar windows are also applied after each AS or VS event (not shown).

Figure A2 illustrates the basic timing concept of pacemaker in (a) DDD mode and (b) DDI mode. DDD mode is an atrial-tracking mode, i.e., pacer's basic interval and AV delay start with each AP or AS. Timeout of the basic interval triggers an AP, and timeout of the AV delay triggers a VP. An AS event detected during the basic interval inhibits the AP, and a VS event detected during the AV delay inhibits the VP. Additionally, a pacer-classified ventricular extra-systole reschedules the next AP at the calculated VA delay. Contrarily, DDI mode is a non-atrial tracking mode. The pacer's basic interval and VA delay starts with each VP or VS. Timeout of the basic interval triggers a VP, and timeout of the VA delay triggers an AP. A VS event detected during the basic interval inhibits the VP, and an AS event detected during the VA delay inhibits the AP.

APPENDIX B: MODEL PARAMETERS

The simulation loads model parameters from an external configuration file. The model parameters are grouped into nine parts, corresponding to the simulation environment and eight model components. Most parameters inherited from the AF–VP model have been described elsewhere,[12,16] whereas those extended heart model parameters and pacer specific model parameters can be understood from the text or comments. An exemplary set of model parameters is listed in Table B1. The parameters that are changed to produce Figs. 6–11 are, respectively, listed in Table B2.

APPENDIX C: MODEL EVENT HANDLING

This section describes the IDHP event handling services shown in Figs. 4 and 5.

TABLE B1. List of an exemplary set of model parameters.

Parameter (unit)	Value	Comments
// Simulation environment parameters		
fnRR	= outrr1.txt	// output RR (VV) interval filename
fnPP	= outpp1.txt	// output PP (AA) interval filename
fnPR	= outpr1.txt	// output PR (AV) interval and AVJ status filename
fnMK	= outmk1.txt	// output event marker filename
fnLOG	= outlog1.txt	// output event log filename
MAX_BEAT	= 10	// max ventricular beats to run
MAX_TIME(s)	= 100	// max simulation time to run
Ts(s)	= 0.001	// sampling interval
RR0(s)	= 1.0	// initial RR interval
// Atrial rhythm generator (ARG) module parameters		
ARG_MODEL	= 3	// 1-exponential, 2-uniform, 3-Gaussion, 4-external, others-fixed
lambda(1/s)	= 1	// mean arrival rate of ARG impulses (mean interval = 60/lambda)
AAstd(s)	= 0.05	// standard deviation of ARG output intervals
dVmean(mV)	= 50	// mean AVJ potential incr. (ΔV) by ARG impulse bombardment
dVstd(mV)	= 0	// standard deviation of ΔV
AES_Prob	= 0.005	// probability of atrial extra-systole (per atrial cycle)
AES_CI1	= 0.2	// shortest possible coupling interval of atrial extra-systole
AES_CT2	= 0.6	// longest possible coupling interval of atrial extra-systole
ANZ_Prob	= 1e−6	// probability of atrial noise (per sample)
// Ventricle rhythm generator (VRG) module parameters		
VRG_MODEL	= 3	// 1-exponential, 2-uniform, 3-Gaussion, 4-external, others-fixed
VVmean(s)	= 3.0	// mean VRG output interval (mean escape rate = 60/VVmean)
VVstd(s)	= 0.05	// standard deviation of VRG output interval
VES_Prob	= 0.005	// probability of ventricular extra-systole (per ventricle cycle)
VES_CI1	= 0.3	// shortest possible coupling interval of ventricular extra-systole
VES_CT2	= 0.6	// longest possible coupling interval of ventricular extra-systole
VNZ_Prob	= 1e−6	// probability of ventricular noise (per sample)
// Atrial conductor module parameters		
AtrAntDly(s)	= 0.03	// antegrade conduction delay from ARG to AVJ
AtrRetDly(s)	= 0.03	// retrograde conduction delay from AVJ to ARG
AtrRef(s)	= 0.05	// atrial refractory period
// Ventricle conductor module parameters		
VtrAntDly(s)	= 0.05	// antegrade conduction delay from AVJ to VRG
VtrRetDly(s)	= 0.1	// retrograde conduction delay from VRG to AVJ
VtrRef(s)	= 0.2	// ventricular refractory period
// AVJ module parameters		
Vt(mV)	= −40	// AVJ excitation threshold potential
Vr(mV)	= −90	// AVJ resting membrane potential
dVdt(mV/s)	= 30	// AVJ spontaneous depolarization slope
MinAVDa(s)	= 0.1	// shortest possible antegrade AV conduction time
MinAVDr(s)	= 0.1	// shortest possible retrograde AV conduction time
alpha(s)	= 0.15	// longest possible extension of AV conduction time
tau_c(s)	= 0.1	// time constant of AV conduction time vs. AVJ recovery time
MinRef(s)	= 0.05	// shortest possible AVJ refractory period
beta(s)	= 0.25	// longest possible extension of AVJ refractory period
tau_r(s)	= 0.5	// time constant of AVJ refractory period vs. AVJ recovery time
Ref_std(s)	= 0	// standard deviation of AVJ refractory period
delta	= 10	// concealed electrotonic modulation affected by impulse strength
theta	= 10	// concealed electrotonic modulation affected by impulse timing
// Atrial lead module parameters		
ApThresh(V)	= 1.0	// atrial pacing threshold
// Ventricle lead module parameters		
VpThresh(V)	= 1.0	// ventricular pacing threshold
// Pacer module parameters		
MODE	= DDD	// pacer mode: DDD, DDI, DVI, VDD, VVI, AAI, VOO, AOO
BI(s)	= 1.0	// standby pacing basic interval (also known as lower rate limit)
AVDp(s)	= 0.18	// paced AV delay (started after each AP in DDD mode)
AVDs(s)	= 0.16	// sensed AV delay (started after each AS in DDD mode)
PVARP(s)	= 0.325	// post-ventricular atrial refractory period
FFWp(s)	= 0.15	// far-field window after ventricular pace

TABLE B1. continued.

Parameter (unit)	Value	Comments
FFWs(s)	= 0.1	// far-field window after ventricular sense
ARP(s)	= 0.3	// pacemaker atrial refractory period
VRP(s)	= 0.25	// pacemaker ventricular refractory period
PVAB(s)	= 0.035	// post-VP atrial blanking window (x-channel VP blanking)
PAVB(s)	= 0.07	// post-AP ventricular blanking window (x-channel AP blanking)
IPAB(s)	= 0.125	// post-AP atrial blanking window (in-channel AP blanking)
IPVB(s)	= 0.11	// post-VP ventricular blanking window (in-channel VP blanking)
ISAB(s)	= 0.125	// post-AS atrial blanking window (in-channel AS blanking)
ISVB(s)	= 0.1	// post-VS ventricular blanking window (in-channel VS blanking)
UTI(s)	= 0.5	// upper tracking interval (upper tracking rate = 60/UTI)
SW(s)	= 0.1	// safety window
AP_AMP(V)	= 3.6	// atrial pacing amplitude
VP_AMP(V)	= 3.6	// ventricular pacing amplitude

TABLE B2. List of model parameter changes from Table B1 to produce Figs. 6–11.

Parameter	Value	Comments
// Parameter changes to produce Fig. 6		
AES_Prob	= 0.1	// increase probability of atrial extra-systole
VES_Prob	= 0.1	// increase probability of ventricular extra-systole
// Parameter changes to produce Fig. 7		
AP_AMP(V)	= 0.5	// sub-threshold AP threshold
// Parameter changes to produce Fig. 8		
ARG_MODEL	= 1	// exponential distribution of AF intervals (arrival rate: Poisson)
lambda(1/s)	= 2.5	// mean arrival rate of AF impulses
dVmean(mV)	= 30	// mean AVJ potential increment by AF bombardment
MODE	= DDI	// DDI (non-atrial tracking) mode
// Parameter changes to produce Fig. 9		
lambda(1/s)	= 2.1	// atrial rate (about 126 beats/min)
MinAVDa(s)	= 0.5	// antegrade AV block (pacemaker dependent)
MinAVDr(s)	= 0.5	// retrograde AV block (no retrograde AS)
AVDp(s)	= 0.12	// shorten AV delay after AP
AVDs(s)	= 0.12	// shorten AV delay after AS
// Parameter changes to produce Fig. 10		
lambda(1/s)	= 2.5	// atrial rate (about 150 beats/min)
VRG_MODEL	= 1	// exponential distribution of ventricular intervals
VVmean(s)	= 0.3	// mean VRG output interval (ventricular rate 200 beats/min)
// Parameter changes to produce Fig. 11		
VES_Prob	= 0.1	// increase probability of ventricular extra-systole
PVARP(s)	= 0.2	// shorten post-ventricular atrial refractory period

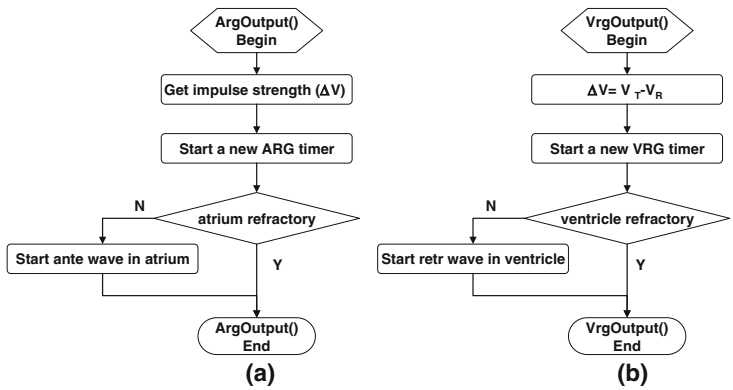

FIGURE C1. The event handling flowcharts for (a) atrial rhythm generator output and (b) ventricle rhythm generator output.

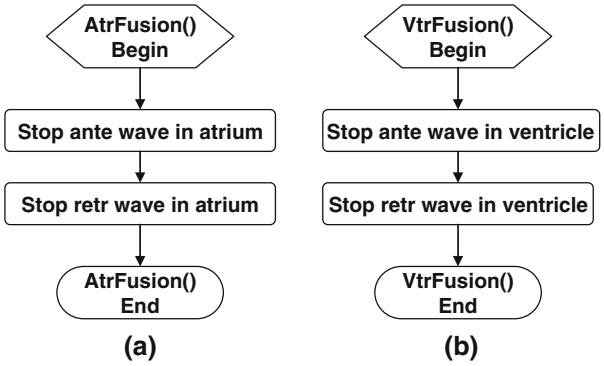

FIGURE C2. The event handling flowcharts for (a) atrial fusion and (b) ventricular fusion.

The *ArgOutput* service is called upon an atrial rhythm generator output (Fig. C1a). The model gets the atrial impulse strength (ΔV) and predicts the arrival time of the next impulse. No atrial depolarization is possible if the atrium is still refractory; otherwise, an antegrade atrial activation wave is generated. The *VrgOutput* service for ventricle rhythm generator output (Fig. C1b) is similarly implemented, except that the ventricular impulse is assumed strong enough that it can bring the AVJ membrane potential (V_m) to the depolarization threshold (V_T).

Atrial fusion (*AtrFusion*) terminates both antegrade and retrograde atrial activation waves (Fig. C2a), and

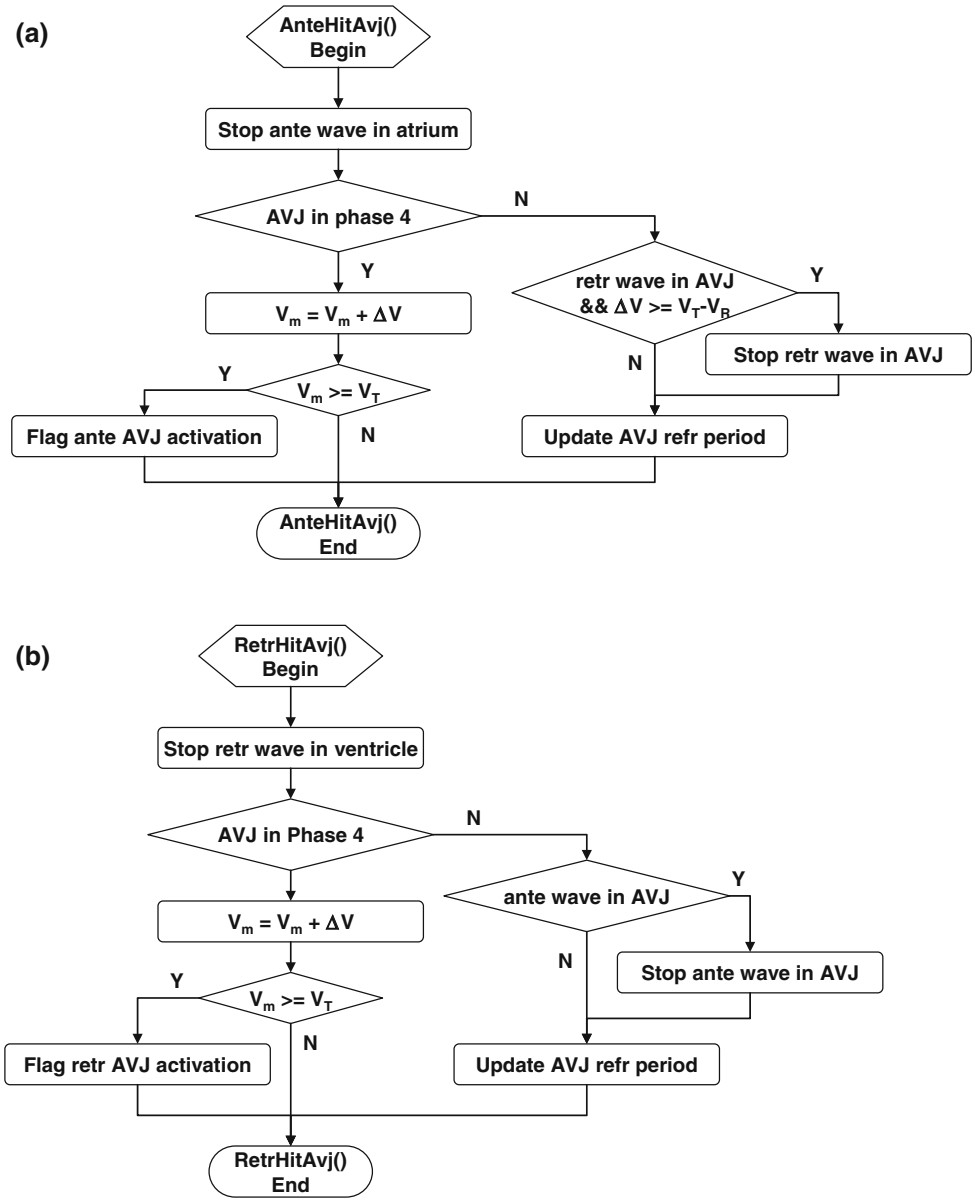

FIGURE C3. The event handling flowcharts for (a) antegrade invasion of AVJ and (b) retrograde invasion of AVJ.

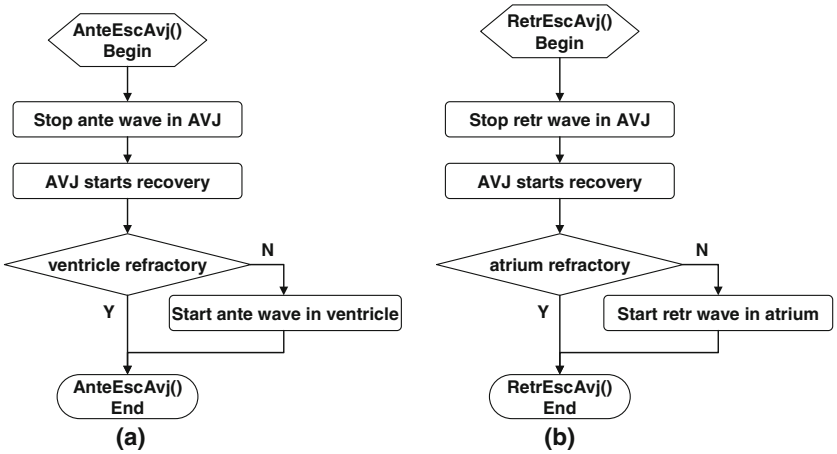

FIGURE C4. The event handling flowcharts for (a) antegrade escaping from AVJ and (b) retrograde escaping from AVJ.

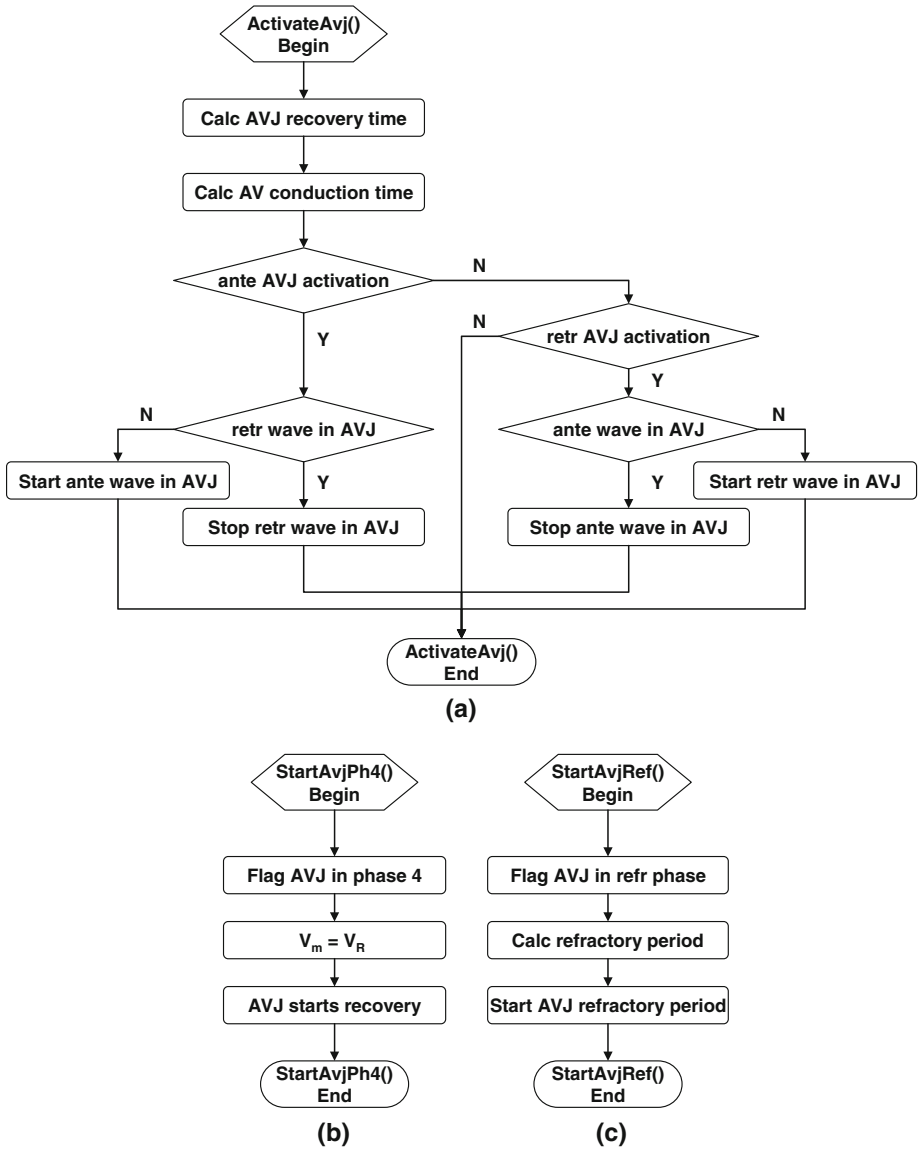

FIGURE C5. The event handling flowcharts for (a) activation of AVJ, (b) start AVJ phase 4, and (c) start AVJ refractory period.

ventricle fusion (*VtrFusion*) annihilates ventricular activation waves in both directions (Fig. C2b).

As shown in Fig. C3a, the antegrade atrial conduction stops when it hits the AVJ (*AntHitAvj*). If AVJ is in phase 4, then V_m has a step increase of ΔV, and antegrade AVJ activation is flagged if $V_m \geq V_T$. If AVJ is still refractory, then its refractory period is extended (electrotonic modulation). If there is a retrograde wave in the AVJ and the atrial impulse has supra-threshold strength, then the retrograde AV conduction is disabled. The counterpart service for retrograde invasion of AVJ (*RetHitAvj*) is similarly implemented (Fig. C3b).

The *AnteEscAvj* service is called upon completion of the antegrade AV conduction (Fig. C4a). It also enables the AVJ for recovery, and starts an antegrade ventricle activation wave if the ventricle is not refractory. Similarly, the *RetrEscAvj* service is implemented (Fig. C4b).

The *ActivateAvj* service (Fig. C5a) is called when $V_m \geq V_T$. It calculates the AV conduction time based on elapsed AVJ recovery time. If the AVJ is antegrade (or retrograde) excited, then an antegrade (or retrograde) AVJ activation wave is generated if there is no activation wave in the opposite direction; otherwise, the opposite activation wave is stopped (AVJ fusion). Start of the AVJ phase 4 (*StartAvjPh4*) resets V_m to the resting potential (V_R) and enables AVJ to recover (Fig. C5b). The *StartAvjRef* service (Fig. C5c) flags the AVJ refractory phase, calculates the refractory period based on the AVJ recovery time, and then starts the AVJ refractory timer.

The *AtrPace* service first checks if the AP amplitude is above the atrial threshold and if the atrium is non-refractory (Fig. C6a). Only if both conditions are met, an antegrade atrial activation wave is generated with supra-threshold strength, and the atrial rhythm generator is reset. Any AP (capture or non-capture) will affect pacer's operation, such as interval measurement, timer update, and marker annotation. Similar implementation of the *VtrPace* service is shown in Fig. C6b.

The *AtrSense* service is called upon detection of any electrical activity by the atrial lead (Fig. C7a). If the sense is caused by retrograde atrial activation, then the atrial rhythm generator is reset. For each atrial sense (excluding blanked ones), pacer will classify its event type, update various counters, timers, intervals, and record the event markers. Similar implementation of the *VtrSense* service is shown in Fig. C7b.

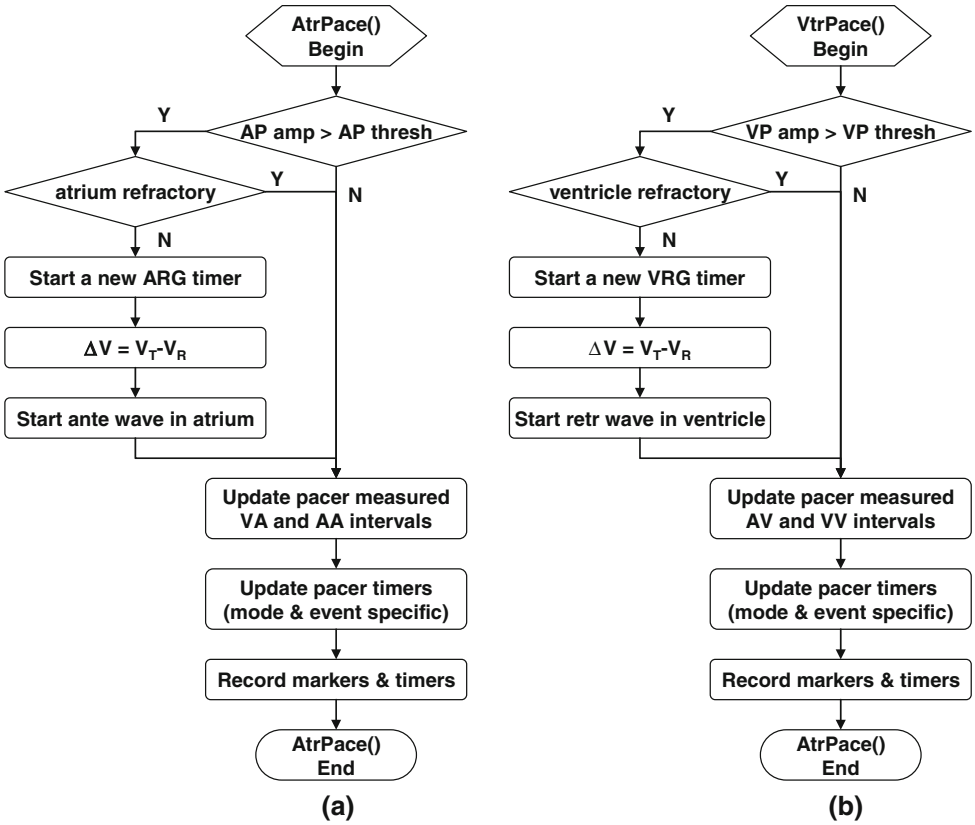

FIGURE C6. The event handling flowcharts for (a) atrial pacing and (b) ventricular pacing.

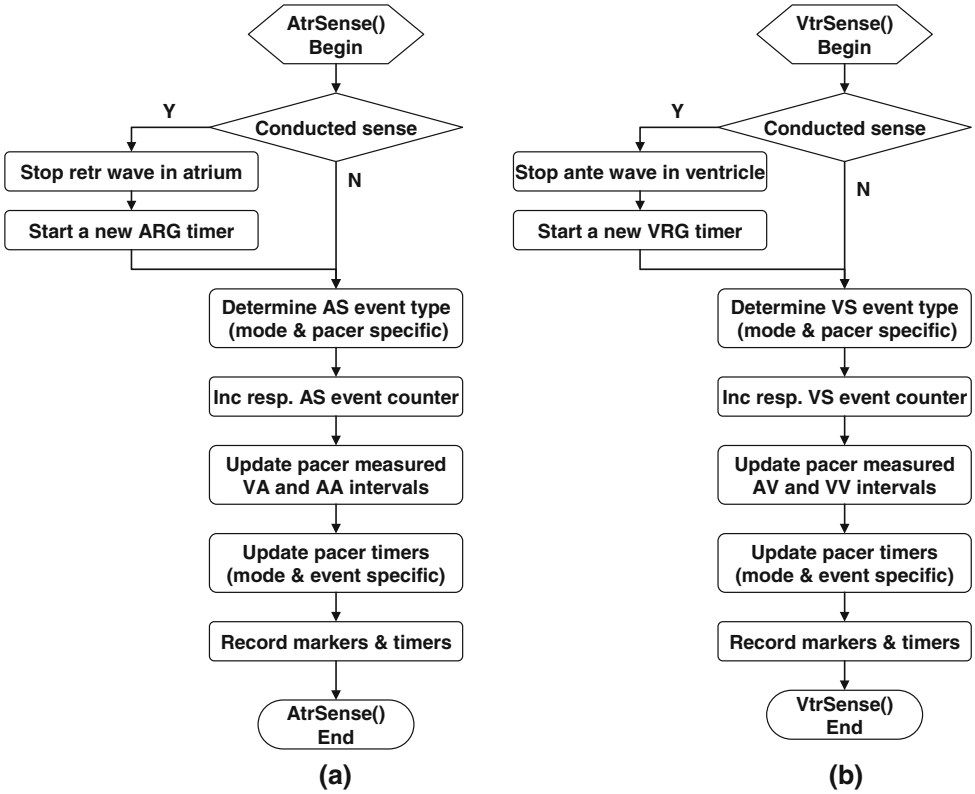

FIGURE C7. The event handling flowcharts for (a) atrial sensing and (b) ventricular sensing.

ACKNOWLEDGMENTS

This work is fully funded by Biotronik GmbH. J. L. and D. M. are both employees of Micro Systems Engineering Inc., a wholly owned subsidiary of Biotronik. Interested readers can contact the authors for using the software program of the present model for research purpose.

REFERENCES

[1]Abraham, W. T., and D. L. Hayes. Cardiac resynchronization therapy for heart failure. *Circulation* 108:2596–2603, 2003. doi:10.1161/01.CIR.0000096580.26969.9A.

[2]Asano, Y., J. Saito, T. Yamamoto, M. Uchida, Y. Yamada, K. Matsumoto, and H. Matsuo. Electrophysiologic determinants of ventricular rate in human atrial fibrillation. *J. Cardiovasc. Electrophysiol.* 6:343–349, 1995. doi:10.1111/j.1540-8167.1995.tb00406.x.

[3]Chorro, F. J., C. J. Kirchhof, J. Brugada, and M. A. Allessie. Ventricular response during irregular atrial pacing and atrial fibrillation. *Am. J. Physiol.* 259:H1015–H1021, 1990.

[4]Cohen, R. J., R. D. Berger, and T. E. Dushane. A quantitative model for the ventricular response during atrial fibrillation. *IEEE Trans. Biomed. Eng.* 30:769–781, 1983. doi:10.1109/TBME.1983.325077.

[5]Ellenbogen, K. A., and M. A. Wood. Cardiac Pacing and ICDs. 4th ed. Malden: Blackwell Publishing, 2005.

[6]Goldberger, A. L., L. A. Amaral, L. Glass, J. M. Hausdorff, P. C. Ivanov, R. G. Mark, J. E. Mietus, G. B. Moody, C. K. Peng, and H. E. Stanley. PhysioBank, PhysioToolkit, and PhysioNet: components of a new research resource for complex physiologic signals. *Circulation* 101:E215–E220, 2000.

[7]Goldstein, R. E., and G. O. Barnett. A statistical study of the ventricular irregularity of atrial fibrillation. *Comput. Biomed. Res.* 1:146–161, 1967. doi:10.1016/0010-4809(67)90013-4.

[8]Heethaar, R. M., J. J. Denier van der Gon, and F. L. Meijler. Mathematical model of A-V conduction in the rat heart. *Cardiovasc. Res.* 7:105–114, 1973. doi:10.1093/cvr/7.1.105.

[9]Heethaar, R. M., R. M. De Vos Burchart, J. J. Denier Van Der Gon, and F. L. Meijler. A mathematical model of A-V conduction in the rat heart. II. Quantification of concealed conduction. *Cardiovasc. Res.* 7:542–556, 1973. doi:10.1093/cvr/7.4.542.

[10]Honzikova, N., B. Fiser, and B. Semrad. Ventricular function in patients with atrial fibrillation. A simulation model study with the aid of a computer. *Cor. Vasa.* 15:257–264, 1973.

[11]Jorgensen, P., C. Schafer, P. G. Guerra, M. Talajic, S. Nattel, and L. Glass. A mathematical model of human atrioventricular nodal function incorporating concealed conduction. *Bull. Math. Biol.* 64:1083–1099, 2002. doi:10.1006/bulm.2002.0313.

[12]Lian, J., D. Müssig, and V. Lang. Computer modeling of ventricular rhythm during atrial fibrillation and ventricular pacing. *IEEE Trans. Biomed. Eng.* 53:1512–1520, 2006. doi:10.1109/TBME.2006.876627.

[13]Lian, J., D. Müssig, and V. Lang. Validation of a novel atrial fibrillation model through simulated atrial pacing protocols. In: *Proceedings of the 28th Annual International Conference of IEEE EMBS*, 2006, pp. 4024–4027.
[14]Lian, J., D. Müssig, and V. Lang. On the role of ventricular conduction time in rate stabilization for atrial fibrillation. *Europace* 9:289–293, 2007. doi:10.1093/europace/eum006.
[15]Lian, J., D. Müssig, and V. Lang. Ventricular rate smoothing for atrial fibrillation: a quantitative comparison study. *Europace* 9:506–513, 2007. doi:10.1093/europace/eum088.
[16]Lian, J., G. Clifford, D. Müssig, and V. Lang. Open source model for generating RR intervals in atrial fibrillation and beyond. *Biomed. Eng. OnLine* 6:9, 2007. doi:10.1186/1475-925X-6-9.
[17]Meijler, F. L., J. Jalife, J. Beaumont, and D. Vaidya. AV nodal function during atrial fibrillation: the role of electrotonic modulation of propagation. *J. Cardiovasc. Electrophysiol.* 7:843–861, 1996. doi:10.1111/j.1540-8167.1996.tb00597.x.
[18]Moe, G. K., and J. A. Abildskov. Observations on the ventricular dysrhythmia associated with atrial fibrillation in the dog heart. *Circ. Res.* 14:447–460, 1964.
[19]Mond, H. G., M. Irwin, C. Morillo, and H. Ector. The world survey of cardiac pacing and cardioverter defibrillators: calendar year 2001. *Pacing Clin. Electrophysiol.* 27:955–964, 2004. doi:10.1111/j.1540-8159.2004.00565.x.
[20]Padeletti, L., F. Fantini, A. Michelucci, P. Pieragnoli, A. Colella, N. Musilli, G. Ricciardi, T. A. Buhr, and S. Valsecchi. Rate stabilization by right ventricular apex or His bundle pacing in patients with atrial fibrillation. *Europace* 7:454–459, 2005. doi:10.1016/j.eupc.2005.05.007.
[21]Talajic, M., D. Papadatos, C. Villemaire, L. Glass, and S. Nattel. A unified model of atrioventricular nodal conduction predicts dynamic changes in Wenckebach periodicity. *Circ. Res.* 68:1280–1293, 1991.
[22]Trohman, R. G., M. H. Kim, and S. L. Pinski. Cardiac pacing: the state of the art. *Lancet* 364:1701–1719, 2004. doi:10.1016/S0140-6736(04)17358-3.
[23]Vereckei, A., Z. Vera, H. P. Pride, and D. P. Zipes. Atrioventricular nodal conduction rather than automaticity determines the ventricular rate during atrial fibrillation and atrial flutter. *J. Cardiovasc. Electrophysiol.* 3:534–543, 1992.
[24]Wittkampf, F. H., and M. J. De Jongste. Rate stabilization by right ventricular pacing in patients with atrial fibrillation. *Pacing Clin. Electrophysiol.* 9:1147–1153, 1985. doi:10.1111/j.1540-8159.1986.tb06685.x.
[25]Wittkampf, F. H., M. J. de Jongste, H. I. Lie, and F. L. Meijler. Effect of right ventricular pacing on ventricular rhythm during atrial fibrillation. *J. Am. Coll. Cardiol.* 11:539–545, 1988.
[26]Zeng, W., and L. Glass. Statistical properties of heartbeat intervals during atrial fibrillation. *Phys. Rev. E* 54:1779–1784, 1996. doi:10.1103/PhysRevE.54.1779.